Genus transition by order shift in a dynamical system

D.E. Rivas-Cisneros*, D.A. Diaz-Romero† and C. Posadas-Castillo‡
Universidad Autónoma de Nuevo León,
San Nicolás de los Garza, Nuevo León, México.
**e-mail: daniel.rivascs@uanl.edu.mx;* †*david.diazrr@uanl.edu.mx;*
‡*cornelio.posadascs@uanl.edu.mx.*

Received 12 November 2019; accepted 11 December 2019

It is well known that the genus of a strange attractor changes if the control parameters of the dynamical system are modified. It is shown that the genus of strange attractors may also depend on the order of the system and that such changes generate different strange attractors. In this work, low-dimensional topological tools are applied in order to know the genus of a strange attractor.

Keywords: Dynamical system; fractional system; attractor; genus; topological surface; canonical form; topological invariant

PACS: 05.45.-a; 05.45.Ac; 05.45.Pq; 02.40.-k; 02.40.Pc; 02.40.Vh DOI: https://doi.org/10.31349/RevMexFis.66.372

1. Introduction

From the topological point of view, strange attractors are classified by their *genus*. Tsankov and Gilmore show a topological tool in [1, 2] that simplifies the calculus of the *genus* for strange attractors. This tool is called the *canonical form* for strange attractors. In integer-order dynamical systems, the topological behavior depends on the control parameters of the system. In [3] it is shown how the genus of the Lorenz attractor can be changed by modification of control parameters.

The theory of integration and differentiation of non-integer order, also called *fractional calculus*, is over 300 years old, but in recent years the number of applications has grown. Fractional calculus allows to consider the integration and derivation of any order, not necessarily integer. This mathematical topic is used in dynamical systems [4], control engineering [5, 6], signal processing [7], statistics [8], among several areas. One of the main reasons that integer-order models were used for a long time, was the absence of solution methods for fractional-order differential equations. Thanks to groundbreaking algorithms such as Caputo, Liouville, Grünwald, Riemann, Letnikov, and enhanced computational resources, it is nowadays feasible to solve fractional-order systems. As a research area it is in continuous development and has several applications, even though, new algorithms are developed to cope with possible downsides of the classical ones, such as [9]. The main advantage of the fractional derivative is the property of memory effect and heredity; these properties provide better information than the integer order derivative. From the applied point of view, fractional order systems behavior is closer to real phenomena found in nature/real world. Physically, the fractional operator takes into account the past and future (memory) of the dynamical system [10, 11].

The change of order does not only affect the chaotic properties of the system, but the topology of the attractor. In [12] it is shown how the surface of a multiscroll Chen attractor changes as well as its genus. In this work, it is shown that by means of order change in the Li and proto-Lorenz attractors, the genus of both systems change, and these changes generate two new strange attractors.

This work is organized as follows: In Sec. 2, the concepts of genus, canonical forms and fractional-order dynamical systems are introduced. In Sec. 3, the integer-order strange attractors of the proto-Lorenz and Li systems are shown. In Sec. 4, the results of order modification for the previous systems are shown. Finally, the conclusion and future work are stated in Sec. 5.

2. Background

This section introduces the theoretical basis on which this work is based.

2.1. Genus, Poincaré surface, first-return map, folding and tearing

Topology is the study of the properties that remain invariant under continuous deformation, one of these properties is the *genus*. The genus g is a *topological invariant* and it is defined as the number of holes on a surface [13]. A topological invariant is defined as a quantity γ that remains unchanged under smooth deformations; if there exist a homeomorphism or diffeomorphism it means that X and Y are *topologically equivalent* if $\gamma(X) = \gamma(Y)$ [14]. For example, the surface of the sphere has $g = 0$ and the surface of the torus $g = 1$; for $g \geq 2$ the surface is the torus with g-holes.

The Poincaré surface and the first-return map are two topological tools that can be used to check whether a strange attractor undergoes changes in its surface; particularly in its genus [3]. For a strange attractor with $g = 1$ the topological process displayed at the first-return map is known as folding, and for $g \geq 3$ the topological process displayed at the first-return map is known as tearing. For more information see [3].

2.2. Canonical forms of strange attractors

As mentioned before, topologically, the strange attractors are classified by their genus. The holes that are generated on the surface of strange attractors are determined by the fixed points of the system [1, 2, 15]. The *canonical form* is the topological tool that helps to know the genus of the strange attractor. This useful tool is defined as the projection of the strange attractor onto a two-dimensional ($x-y$ plane) planar surface with g-interior holes [1, 2]. There are two types of canonical forms that represent the surfaces of a variety of strange attractors. The first is the *chain* A_n $(n \geq 1)$ with n holes-scrolls and $n-1$ separating holes with four singularities each. The genus of this canonical form is $g = 2n-1$, where n is the number of holes-scroll. The second is the *cycle* C_n $(n \geq 2)$ with n holes-scrolls and one hole with $2n$ singularities. The genus of this canonical form is $g = n+1$,

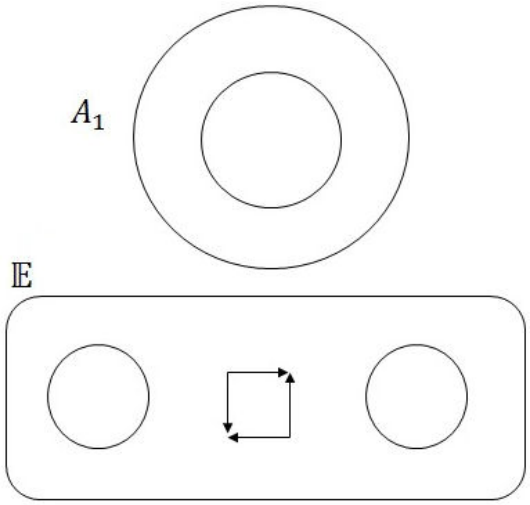

FIGURE 1. A_1 depicts 1-scroll attractors with $g = 1$, where there is a hole without singularities. $\mathbb{E}$ depicts attractors with $g = 3$, where the attractor has 2-scrolls and one hole with four singularities.

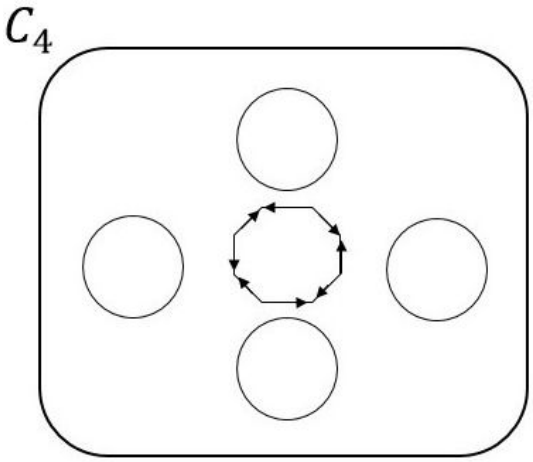

FIGURE 2. C_4 depicts attractors with $g = 5$, where the attractor has 4-scrolls and one hole with eigth singularities.

where n is the number of holes-scroll [1, 2]. Specifically, the A_2 is equal to C_2 [1, 2], then $\mathbb{E} = A_2 = C_2$. Figure 1 shows the canonical form A_1 and $\mathbb{E}$, as well as Fig. 2 shows the canonical form C_4.

2.3. Fractional-order dynamical systems

The fundamental operator of fractional calculus is ${}_aD_t^\alpha$, where a and t are the bounds of the operation and $\alpha \in R$. The operator is defined as [16]:

$$ {}_aD_t^\alpha = \begin{cases} \frac{d^\alpha}{dt^\alpha}, & \alpha > 0 \\ 1, & \alpha = 0 \\ \int_a^t (d\tau)^\alpha & \alpha < 0 \end{cases} $$

For $\alpha = r$ where r is integer, the operation ${}_0D_t^\alpha f(t)$ gives the same results as classical differentiation and integration of integer-order operators. The most used approaches to define the fractional operator are the Grünwald-Letnikov (G-L), Riemann-Liouville (R-L), and Caputo. These definitions are described as follows [16]:

- **Grünwald-Letnikov**

$$ {}_aD_t^\alpha f(t) = \lim_{h\to 0} \frac{1}{h^\alpha} \sum_{j=0}^{\frac{t-a}{h}} (-1)^j \binom{\alpha}{j} f(t-jh). \quad (1) $$

- **Riemann-Liouville**

$$ {}_aD_t^{-\alpha} f(t) = \frac{1}{\Gamma(-\alpha)} \int_a^t \frac{f(\tau)}{(t-\tau)^{\alpha+1}} d\tau. \quad (2) $$

$$ {}_aD_t^\alpha f(t) = \frac{1}{\Gamma(n-\alpha)} \frac{d^n}{dt^n} \int_a^t \frac{f(\tau)}{(t-\tau)^{\alpha-n+1}} d\tau. \quad (3) $$

- **Caputo**

$$ {}_aD_t^\alpha f(t) = \frac{1}{\Gamma(n-\alpha)} \int_a^t \frac{f^{(n)}(\tau)}{(t-\tau)^{\alpha-n+1}} d\tau. \quad (4) $$

In this work, the G-L approximation will be used for the numerical simulation of the systems.

An integer-order dynamical system can be generally defined by a set of first-ordinary differential equations of the form [17]:

$$ \frac{d^r x_i}{dt^r} = F_i(x) \qquad r = 1; \quad i = 1, \ldots, n, \quad (5) $$

where $x = (x_1, x_2, \ldots x_n)$ are the *state variables* and $(c_1, c_2, \ldots c_k)$ are the control parameters of the system. From a topological point of view, a dynamical system consists of a topological space Σ also called *surface*, a time $t \in R$ and an evolution operator $\Phi : \Sigma \times R \to \Sigma$ [18]. In these types of

systems, the topology of Σ depends on the control parameters [17].

A fractional-order dynamical system is an extension of the definition of integer-order dynamical system. It is defined as a set of non-integer order differential equations and is described as follows [19]:

$$ {}_0D_t^{\alpha} x_i = F_i(x;c), \qquad 0 < \alpha \leq 2; \quad i = 1, \ldots, n. \tag{6} $$

Similarly, this system consists of a surface β, a time $t \in R$ and an evolution $\psi : \beta \times R \rightarrow \beta$. In these types of systems, the topology of β depends on the order of the system, as shown in [12].

In fractional-order dynamical systems, the concept of "system order" is not stated as in the integer-order dynamical-systems case. In integer-order dynamical systems, the order of the system is equal to the number of states or set of first-order ordinary differential equations of the system. In fractional-order dynamical systems, the order of the system is equal to the sum of the orders of the differential equations that conform the system. This means, if we have a dynamical system of order 3 which is composed of three first-ordinary differential equations, this can be modified to a system where the differential equations are fractional order derivatives, hence, the order of the system is $2 + \alpha$, where $0 < \alpha \leq 2$ [20] if the three differential equations are of fractional-order, the total order is $\alpha_1 + \alpha_2 + \alpha_3$. In fractional systems the derivative can adopt any arbitrary real value order. A system with constant order, *i.e.* $\alpha_1 = \alpha_2 = \ldots \alpha_i$ is known as a commensurate order. Whilst a system with diverse orders within, *i.e.* $\alpha_1 \neq \alpha_2 \neq \ldots \alpha_i$ is known as an incommensurate order system [21].

The algorithm to solve equation (6) uses the *short memory* principle and is based in the G-L definition (1), the numerical scheme has the following form [16],

$$ {}_{(k-Lm/h)}D_{tk}^{\alpha} f(t) \approx h^{-\alpha} \sum_{j=0}^{k} (-1)^j \binom{\alpha}{j} f(t - jh), \tag{7} $$

where Lm is the *memory length*, $tk = (k = 1, 2, \ldots)$, h is the time step of calculation and $(-1)^j \binom{\alpha}{j}$ are binomial coefficients $c_j^{(\alpha)} (j = 0, 1, \ldots)$. For their calculation the following expression is used [16]:

$$ c_j^{(\alpha)} = \left(1 - \frac{1+\alpha}{j}\right) c_{j-1}^{(\alpha)}. \tag{8} $$

The general numerical solution of the fractional differential equation is as follows:

$$ {}_aD_t^{\alpha} x(t) = f(x(t), t), \tag{9} $$

the solution to wich can be expressed as [16]

$$ x(tk) = f(x(tk), tk) h^{\alpha} - \sum_{j=v}^{k} c_j^{(\alpha)} x(tk - j). \tag{10} $$

According to the literature [10, 16], the G-L approach is equivalent to the R-L and Caputo approaches. The time domain methods to simulate fractional-order systems, require higher computational cost, but are more accurate. The G-L approach has the property of short memory which reduces the computational cost. Nevertheless, this approach has the same reliability and accuracy [10] to simulate fractional-order system as time domain methods.

3. The integer-order attractors

The Li attractor and the proto-Lorenz attractor are presented with their canonical forms.

3.1. The Li attractor

The Li attractor is given by [23]:

$$ \begin{aligned} \dot{x} &= a(y - x) + dxz, \\ \dot{y} &= kx + fy - xz, \\ \dot{z} &= cz + xy - ex^2, \end{aligned} \tag{11} $$

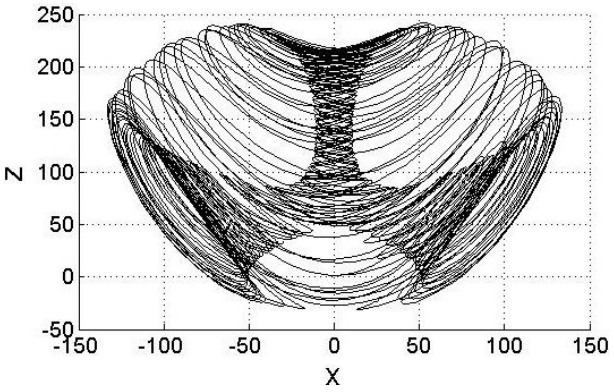

FIGURE 3. Simulation result onto $x - z$ plane of the system (11) with $a = 40$, $c = 11/6$, $d = 0.16$, $e = 0.65$, $k = 55$, $f = 20$; and initial conditions $(x_0, y_0, z_0) = (1.5, 1.5, 1.5)$.

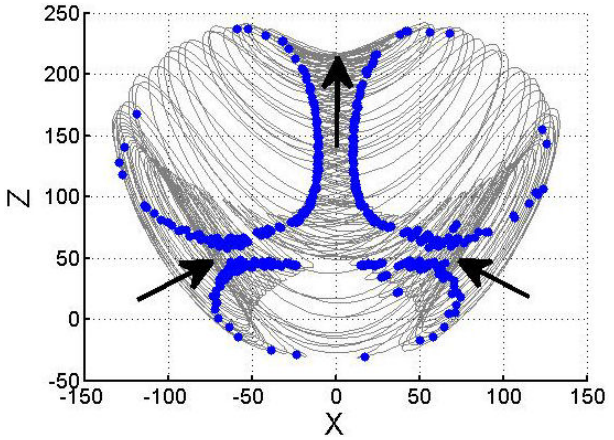

FIGURE 4. Poincaré section spliced with Li's attractor trajectories.

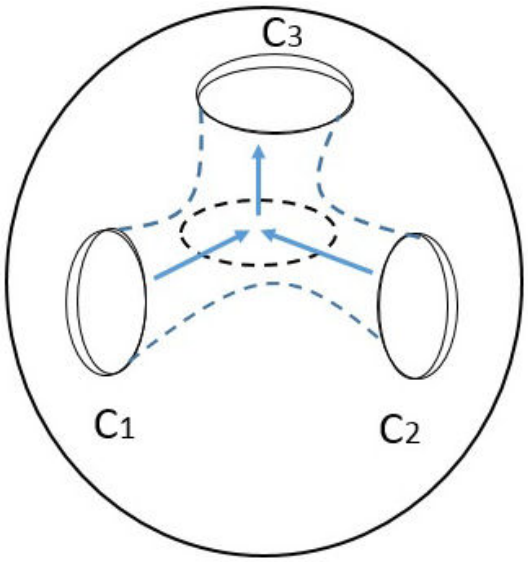

FIGURE 5. Explanatory diagram of the Li attractor.

where the parameters of the system are: $a = 40$, $c = 11/6$, $d = 0.16$, $e = 0.65$, $k = 55$, $f = 20$.

Topologically, Letellier and Gilmore in [15] define this attractor as a solid sphere pierced by two intersecting scrolls at symmetry axis, and they conclude that the genus of the attractor is 3. Therefore, its canonical form is $\mathbb{E}$. The Fig. 3 shows the integer-order Li attractor of the Eq. (11) with the projection onto the $x - z$ plane. Figure 4 shows the Poincaré section with blue color and Li's attractor trajectories with gray color, which are spliced to show the three holes (three scrolls), the holes are pointed out by black arrows. The Fig. 5 shows an explanatory diagram where C1 and C2 are the holes that are generated in the Li attractor and the intersection of C1 and C2 generate the third hole C3.

3.2. The integer-order proto-Lorenz attractor

The proto-Lorenz attractor with 4-scrolls is given by [22]:

$$\begin{aligned}\dot{s} &= \frac{1}{2(s^2+w^2)} f(x),\\ \dot{w} &= \frac{1}{2(s^2+w^2)} f(w),\\ \dot{z} &= 2s^3 w - 2sw^3 - bz, \end{aligned} \tag{12}$$

where $f(x) = [-as^3 + (2a + c - z)s^2 w + (a - 2)sw^2 - (c - z)w^3]$ and $f(w) = [(c - z)s^3 + (a - 2)s^2 w + (-2a - c + z)sw^2 - aw^3]$. The control parameters are: $(a, b, c) = (10, 8/3, 28)$. The Fig. 6 shows the 4-scrolls strange attractor in R^3 of the system (12) and the Fig. 7 shows the projection onto $x - y$ plane of the system (12).

The Fig. 7 clearly shows that the attractor has 4 scrolls, according to [1, 2], the canonical form that depicts this attractor is the C_4. The Fig. 2 shows this canonical form, the attractor has 4-scrolls and one hole with eight $(2n)$ singularities. Using the expression $g = n + 1$, we have that $g = 5$.

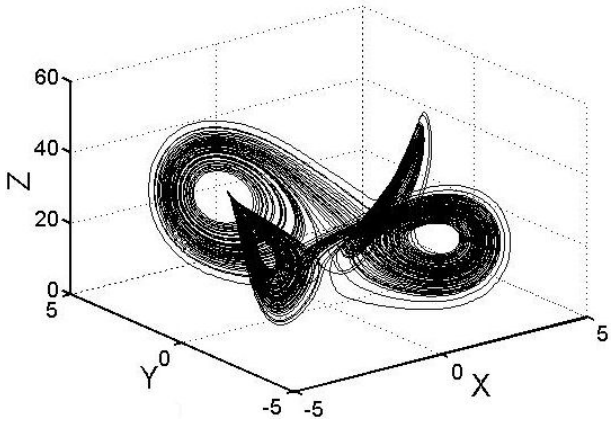

FIGURE 6. 4-scroll strange attractor in R^3 of the system (12), with $(a, b, c) = (10, 8/3, 28)$ and initial conditions $(s_0, w_0, z_0) = (1, 2, 6)$.

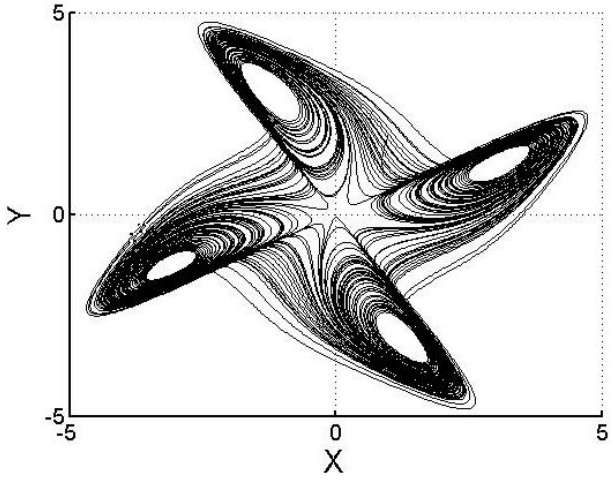

FIGURE 7. Projection onto $x - y$ plane for the 4-scroll strange attractor generated by system (12), with $(a, b, c) = (10, 8/3, 28)$ and initial conditions $(s_0, w_0, z_0) = (1, 2, 6)$.

4. Results

In this section the genus change for the previously stated attractors is presented. This change surfaces as the order of the system is modified. In these results, the parameters of the systems remain constant through all cases.

4.1. Fractional-order Li attractor

According to Eq. (6) the fractional-order Li system is defined as follows:

$$\begin{aligned} D_t^{\alpha_1} x &= a(y - x) + dxz\\ D_t^{\alpha_2} y &= kx + fy - xz\\ D_t^{\alpha_3} z &= cz + xy - ex^2, \end{aligned} \tag{13}$$

where the parameters and initial conditions are the same as those of the integer-order system. The order of the system

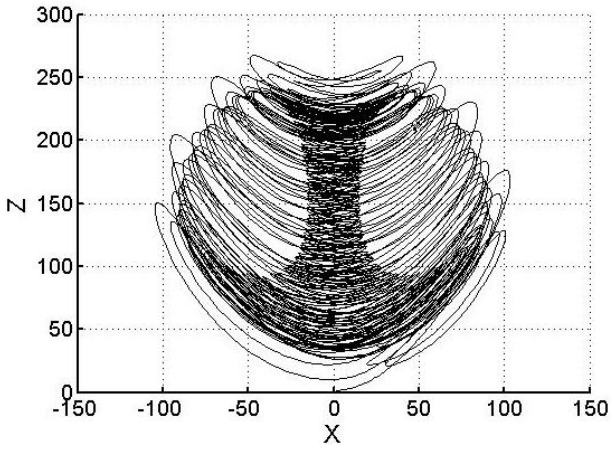

FIGURE 8. Simulation result projection onto $x-z$ plane with order $(\alpha_1, \alpha_2, \alpha_3) = (1, 0.9, 1)$.

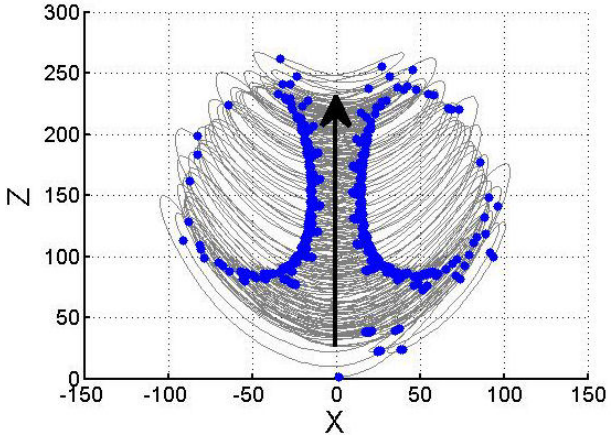

FIGURE 9. Poincaré section of the new 1-scroll attractor spliced with the trajectories of the system (13).

α is the only parameter that changes, with incommensurate order $(\alpha_1, \alpha_2, \alpha_3) = (1, 0.9, 1)$. In Fig. 6, the new 1-scroll strange attractor generated by system 13 is shown, Fig. 9 shows the Poincaré section in blue color and trajectories of the system (13) in gray color, which are spliced in order to show the 1-hole generated within the new attractor; the hole is indicated with a black arrow. Figure 10 depicts an explanatory diagram where C1 and C2 holes come together making a single hole which connects to the C3 hole, generating a single hole or scroll.

It is clearly observed that the number of scrolls changes respect to system (11). This attractor has 1-scroll and belongs to the canonical form A_1, using the expression $g = 2n - 1$ the resulting genus is $g = 1$.

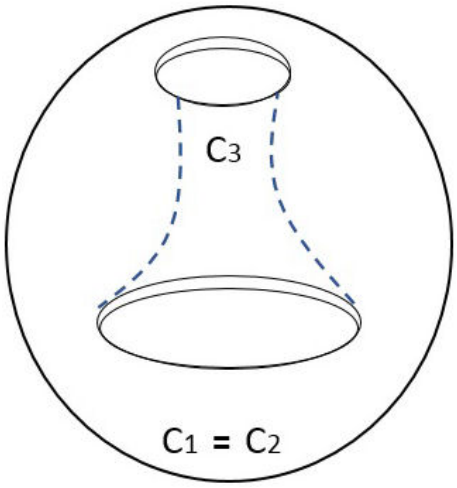

FIGURE 10. Explanatory diagram of the system (13).

4.2. Fractional-order proto-Lorenz attractor

According to the Eq. (6) the fractional-order proto-Lorenz system is defined as follows:

$$\begin{aligned} D_t^{\alpha_1} s &= \frac{1}{2(s^2+w^2)} f(x), \\ D_t^{\alpha_2} w &= \frac{1}{2(s^2+w^2)} f(w), \\ D_t^{\alpha_3} z &= 2s^3 w - 2sw^3 - bz, \end{aligned} \tag{14}$$

where $f(x) = [-as^3 + (2a + c - z)s^2 w + (a - 2)sw^2 - (c - z)w^3]$ and $f(w) = [(c - z)s^3 + (a - 2)s^2 w + (-2a - c + z)sw^2 - aw^3]$. The control parameters and the initial conditions are the same as for the system (12). With order $(\alpha_1, \alpha_2, \alpha_3) = (1.15, 0.7, 1.15)$, the system (14) generates a new 2-scroll strange attractor, as shown in Fig. 11.

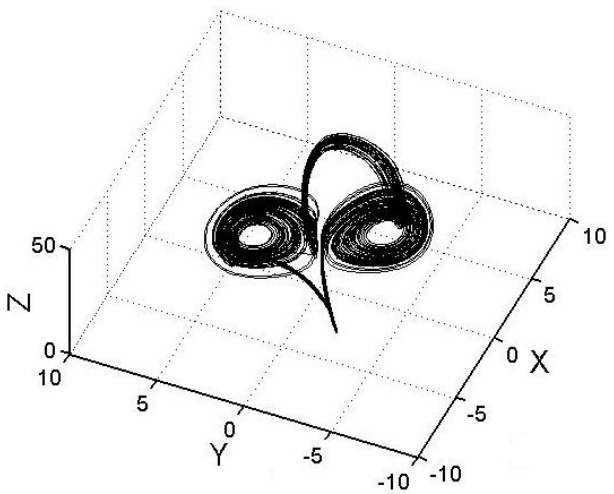

FIGURE 11. Simulation result of system (14) in R^3 with $\alpha_1 = 1.15$, $\alpha_2 = 0.7$, and $\alpha_3 = 1.15$.

It is clearly observed that the number of scrolls changes with respect to system (12). This attractor has 2-scroll trajectory, as mentioned before $A_2 = C_2$, using the expressions $g = 2n - 1$ and $g = n + 1$ the result is $g = 3$ therefore, its canonical form is $\mathbb{E}$.

Please notice that in the results for the fractional-order Li and Proto-Lorenz attractors, the only modified value is the order of the system. Parameters and initial values remain the same.

5. Conclusions

A change in the order of a fractional dynamical system may modify its topology and it may even generate new strange attractors. In this work we show two cases of such behavior.

As a future work it is proposed to analyze the fixed points of the systems to know the process of genus modification of the attracor.

As stated, smooth changes in the order of the system have strong implications for the dynamical behavior and the structure of the system, hence, the change of genus occurs in the "new" system.

Previous works analyze characteristics of the system under order variation, but these works do not address the topological aspect [16]. The present results widen the set of possible tools to analyze fractional-order systems under soft order variation and its implications.

Possible applications of these results may be on the analysis of bifurcations for fractional order dynamical systems under smooth order change.

The downfalls that might affect some analyses may be the simulations of the dynamical systems, however, as we are using topological tools, these pitfalls can be avoided.

Acknowledgments

The authors thank to CONACYT for its support.

1. T. D. Tsankov and R. Gilmore, *Phys. Rev. Lett.* **91** (2003) 134104. https://doi.org/10.1103/PhysRevLett.91.134104
2. T. D. Tsankov and R. Gilmore, *Phys. Rev. E* **69** (2004) 056206. https://doi.org/10.1103/PhysRevE.69.056206
3. C. Letellier, T. D. Tsankov, G. Byrne and R. Gilmore, *Phys. Rev. E* **72** (2005) 026212. https://doi.org/10.1103/PhysRevE.72.026212
4. M. S. Tavazoei and M. Heari, *Nonlinear Anal.* **69** (2008) 1299. https://doi.org/10.1016/j.na.2007.06.030
5. I. Petráš, *J. Electr. Eng.* **60** (2009) 117. http://iris.elf.stuba.sk/JEEEC
6. L. F. Ávalos-Riuz, C. J. Zúñiga-Aguilar, J. F. Gómez-Aguilar, R. F Escobar-Jimenez, and H. M. Romero-Ugalde, *Solitons Fract.* **115** (2018) 177. https://doi.org/10.1016/j.chaos.2018.08.021
7. H. Sheng, Y. Q. Chen and T. S. Qiu, *Fractional Processes and Fractional-Order Signal Processing*, (Signals and Communication Technology, Springer, 2011) pp. 31. https://doi.org/10.1007/978-1-4471-2233-3
8. A. Atangana and J. F. Gómez-Aguilar, *Chaos, Solitons Fract.* **114** (2018) 516. https://doi.org/10.1016/j.chaos.2018.07.033
9. A. Atangana and J. F. Gómez-Aguilar, *Phys. A* **476** (2017) 1. https://doi.org/10.1016/j.physa.2017.02.016
10. I. Podlubny, *Fractional Differential equation* (Academic Press, 1999)
11. J. F. Gómez-Agular, *Numer. Meth. Part. D. E.* **34** (2018) 1716. https://doi.org/10.1002/num.22219
12. D. E. Rivas-Cisneros, D.A. Díaz-Romero, *Memorias del Congreso Nacional de Control Automático* (2016). http://amca.mx/memorias/amca2016
13. P. R. Cromwell, *Knots and Links*, (1st ed. Cambridge University Press, 2004) pp. 38. https://doi.org/10.1017/CBO9780511809767
14. L. C. Kinsey, *Topology of Suerfaces*, (1st ed. Springer, 1993) pp. 94. https://doi.org/10.1007/978-1-4612-0899-0
15. T. D. Letellier and R. Gilmore, *J. Phys. A: Math. Theor.* **42** (2009) 015101. https://doi.org/10.1088/1751-8113/42/1/015101
16. I. Petráš, *Fractional-Order Nonlinear Systems: Modeling, Analysis and Simulation*, (Nonlinear Physical Science, Springer, 2011) pp. 7. https://doi.org/10.1007/978-3-642-18101-6
17. R. Gilmore and M. Lefranc, *The Topology of Chaos: Alice in Stretch and Squeezeland*, (Wiley-Interscience, 2002) pp. 97. https://doi.org/10.1002/9783527617319
18. H. Broer and F. Takens, *Dynamical Systems and Chaos*, (**Vol. 172**, Springer, 2011) pp. 133. https://doi.org/10.1007/978-1-4419-6870-8
19. V. E. Tarasov, *Fractional Dynamics: Applications of Fractional Calculus to Dynamics of Particles, Fields and Media* (Nonlinear Physical Science, Springer, 2010) pp. 293. https://doi.org/10.1007/978-3-642-14003-7
20. I. Petráš, *Control of fractional-order Chua's system*, ePrint: arXiv:nlin/0008029[nlin.CD]
21. M. S. Tavazoei and M. Heari, *Phys. D* **237** (2008) 2628. https://doi.org/10.1016/j.physd.2008.03.037
22. J. HÜ and G. Chen, *Int. J. Bifurcat. Chaos* **16** (2006) 775. https://doi.org/10.1142/S0218127406015179
23. D. Li, *Phys. Lett. A* **372** (2008) 387. https://doi.org/10.1016/j.physleta.2007.07.045